Catalysis Science & Technology

PAPER

View Article Online
View Journal | View Issue

Cite this: *Catal. Sci. Technol.*, 2014, **4**, 729

Application of halohydrocarbons for the re-dispersion of gold particles†

Kevin Morgan,[a] Robbie Burch,[a] Muhammad Daous,[b] Juan José Delgado,[c] Alexandre Goguet,[a] Christopher Hardacre,*[a] Lachezar A. Petrov[d] and David W. Rooney[a]

Received 11th November 2013,
Accepted 20th December 2013

DOI: 10.1039/c3cy00915g

www.rsc.org/catalysis

Methods to control the dispersion of gold in supported heterogeneous catalysts are very valuable due to the strong nanoparticle size dependence on their activity and selectivity towards many reactions. Additionally, the ability to disperse large, inactive gold nanoparticles to smaller nanoparticles provides an opportunity to reactivate, stabilise and increase the lifetime of gold catalysts making them more practical for industrial applications. Previously it has been demonstrated that the use of gas phase iodomethane (*J. Am. Chem. Soc.*, 2009, **131**, 6973; *Angew. Chem., Int. Ed.*, 2011, **50**, 8912) was able to re-disperse gold from >20 nm particles to dimers and trimers. In the current work, we show that this technique can be applied using less hazardous halohydrocarbons treatments, both in the gas phase and the liquid phase. The ability of these individual halohydrocarbons to re-disperse gold as well as the extent to which leaching occurs is assessed.

Introduction

Gold is no longer seen as a catalytically inert material and the ability to produce small nanoparticles of gold has led to the discovery of active gold catalysts. There has been increasing interest in processes relating to catalytically active gold[1] since it was first reported to be active for CO oxidation and hydrochlorination of acetylene in the 1980s.[2,3] Since then, a wide range of processes have been explored for Au based catalysis including hydrogenations, epoxidations and selective oxidations and applied in sectors as varied as environmental remediation to bulk and pharmaceutical chemical production.[1,4]

Although these systems have been shown to be highly active and selective in many cases, Au based catalysts have a tendency to have low stability. Under reaction conditions and/or thermal treatment, gold catalysts are found to undergo irreversible deactivation.[5] Various deactivation mechanisms have been proposed including sintering of the gold, and there is generally a strong correlation between the gold nanoparticle size and catalyst activity.[1,5–8] Hence, methods which can re-disperse gold from large to smaller nanoparticles would have a major application in the reactivation of gold catalysts, thereby making such materials more likely to become viable and practical industrial catalysts.

Recently, it has been reported that during the gold catalyzed carbonylation of methanol to methyl acetate in the presence of iodomethane, large gold nanoparticles (~20 nm) were dispersed forming stable gold dimers and trimers.[4,9] Whilst these observations showed that it was possible to re-disperse gold nanoparticles, the conditions were too harsh (240 °C and 16 bar pressure) to provide a practical procedure for this to be used routinely with other supported gold catalysts. Further studies indicated that milder CH_3I treatments (at atmospheric pressure) of gold supported on both carbon and metal oxides were able to re-disperse the gold particles down to the atomic level.[1,5] Importantly, a range of gold loadings was able to be dispersed from 0.8 wt.% to 2.0 wt.% Au supported on carbon and metal oxides demonstrating the general applicability of the treatment. Some variations were observed between the supports, however, showing that the gold-support interaction is important in determining the final state of the catalyst following treatment. In the previous studies, the proposed mechanism for the dispersion was the oxidation of gold through interaction with iodine followed by dissociation of these Au–I species from the gold nanoparticle.[1,5] Whilst mild conditions could be employed, these still required the use of CH_3I. Iodomethane is toxic[10,11] and is

[a] *CenTACat, School of Chemistry and Chemical Engineering, Queen's University, Belfast, BT9 5AG, Northern Ireland, UK. E-mail: c.hardacre@qub.ac.uk*
[b] *Chemical and Materials Engineering Department, King Abdulaziz University, Jeddah, Saudi Arabia*
[c] *Departamento de Ciencia de los Materiales e Ingeniería Metalúrgica y Química Inorgánica de la Universidad de Cádiz, Puerto Real, Cádiz, Spain*
[d] *SABIC Chair of Catalysis, Chemical and Materials Engineering Department, King Abdulaziz University, Jeddah, Saudi Arabia*

† Electronic supplementary information (ESI) available. See DOI: 10.1039/c3cy00915g

Table 1 Price per mL of halohydrocarbons

Compound	Price per mL
Iodomethane	£0.57
n-Iodobutane	£0.20
n-Iodohexane	£0.42
n-Iodooctane	£0.40
p-Iodotoluene	£0.77
n-Bromobutane	£0.04
n-Bromohexane	£0.09
n-Bromooctane	£0.10
p-Bromotoluene	£0.21

a carcinogen;[12] hence, it would be beneficial if a similar dispersion effect could be observed using other halo compounds with lower toxicity.[13]

This paper reports the use of bromo- and iodohydrocarbons (RX) to determine the effect of increasing carbon chain length and the effect of aromatic *versus* aliphatic molecules for the dispersion of large gold particles. The overall aim was to examine whether milder, safer treatments for this process could be obtained compared with the CH_3I process. Both gas phase and liquid phase treatments have been studied to allow direct comparison with the previously reported method.[1,5] Additionally, many of the alternative halohydrocarbons are cheaper than iodomethane. Table 1 compares commercial list prices per mL of the halohydrocarbons used in this study.[14]

Experimental

Materials

The catalyst used for this study was 1 wt.% Au/C supplied by the World Gold Council and was used as received. Hexane, iodomethane, *n*-iodobutane, *n*-iodohexane, *n*-iodooctane, *n*-bromobutane, *n*-bromohexane, *n*-bromooctane, *p*-iodotoluene, *p*-bromotoluene, acetonitrile and toluene of AR grade were obtained from Sigma–Aldrich and were used without further purification. Distilled deionised water was used where indicated. Argon (99% purity) was obtained from BOC.

Gas phase haloalkane treatments

All gas phase treatments using bromo- and iodoalkanes (RX) were performed in a quartz reactor (O.D. 10 mm) using *ca.* 100 mg of catalyst and a steady flow of 40 cm^3 min^{-1} of RX/Ar. The quartz reactor was heated in a tubular furnace under a flow of argon and the temperature was increased to the set temperature (240 °C) using a ramp rate of 10 °C min^{-1} followed by a dwell at this set temperature of 1 h. Once at temperature, the RX/Ar was admitted to the reactor.

The amount of RX in the feed was controlled by the vapour pressure (calculated from the Antoine equation), which was determined by a saturator held at 25 °C in most cases. The vapour pressure and volumetric flow rates of the respective species are reported in Table 2. After treatment, the sample was cooled under argon (40 cm^3 min^{-1}) and later transferred to a sealed sample vial.

Table 2 Vapour pressures and volumetric flow rates of iodoalkanes at 25 °C

Compound	Vapour pressure (kPa)	Volumetric flow rate (cm^3 min^{-1})
Iodomethane	53.30	0.1400
n-Iodobutane	22.36	0.0587
n-Iodohexane	0.26	0.0007
n-Iodooctane[a]	0.29	0.0008
n-Bromobutane	4.48	0.0118
n-Bromohexane[b]	0.42	0.0011
n-Bromooctane[c]	0.35	0.0009

Saturator at [a] 60 °C, [b] 50 °C and [c] 80 °C.

In the case of *n*-iodooctane, *n*-bromohexane and *n*-bromooctane the treatment conducted with the saturator held at 25 °C was found to be ineffective due to the very low vapour pressure of the reactant. Therefore, in the case of *n*-iodooctane, *n*-bromohexane and *n*-bromooctane the reported results are from treatments with the saturator heated to 60, 50 and 80 °C, respectively. At these temperatures, the concentration in the feed was similar to or greater than that of *n*-iodohexane with the saturator held at 25 °C.

Pure liquid phase halohydrocarbon treatments

4 cm^3 of halohydrocarbon (RX) was added to a sealed sample vial with 100 mg of catalyst. The samples were heated to 40 °C to ensure that all the materials used were liquid as the halotoluenes are solid at room temperature. The samples were stirred vigorously using a magnetic stirrer at temperature 1 h. After treatment, the samples were filtered, washed with distilled water and dried before being stored in sealed sample vials.

Dilute liquid phase halohydrocarbon treatments

The RX (0.2 cm^3) was dissolved in 4 cm^3 of hexane and mixed with 100 mg of catalyst at room temperature, in a sealed sample tube and was magnetically stirred for 24 h. After treatment, the samples were filtered, washed with distilled water and dried before being stored in sealed sample vials. In the case of the diluted *n*-iodooctane, this procedure was repeated for samples stirred for 2, 4, 6, 8, 12, 16, 20 and 24 h. GC/MS analysis of the liquid phase following the treatment of the catalyst was undertaken using an AutoSystem XL GC (Perkin Elmer) coupled with a TurboMass MS (Perkin Elmer).

Characterisation

Powder X-Ray diffraction (PXRD) measurement was carried out using a PANalytical X'Pert Pro X-ray diffractometer. The X-ray source used was copper K_α with a wavelength of 1.5405 Å. Diffractograms were collected from 20° to 85° with a step size of 0.04°. The full width half maximum values quoted in the paper are reported with a variance of ±0.04°.

The preparation of samples for inductively coupled plasma–optical emission spectrometry (ICP-OES) consisted of ashing

followed by digestion with aqua reggia. A Perkin Elmer 4300 DV ICP-OES was used to quantify the amount of gold for all the catalysts.

High Resolution Transmission Electron Micrographs were collected on a 200 kV JEOL JEM-2010F instrument with a structural resolution of 0.19 nm at Scherzer defocus conditions. Scanning Transmission Electron Microscopy (STEM) images were recorded in the same instrument using a high-angle annular dark-field (HAADF) detector and an electron beam probe of 0.5 nm to determine the particle size distribution and the metal dispersion assuming a cubooctahedric shape. This analysis was performed by counting up to 400 particles.

Results and discussion

Gas phase haloalkane treatments

Fig. 1 reports the diffractograms of the as received Au/C catalyst, as well as the samples treated with iodomethane, *n*-iodobutane, *n*-iodohexane and *n*-iodooctane for 1 h at 240 °C. Diffraction features associated with gold are clearly observed in the case of the as received catalyst with the Au(111) at 38.4°, Au(200) at 44.6°, Au(220) at 64.8°, Au(311) at 77.7° and Au(222) at 81.8°. After treatment with the iodoalkanes, significant changes are observed. In all cases, the treatment with the iodo compounds resulted in the disappearance of all the gold diffraction features. This is consistent with a decrease in gold particle size due to the treatment with the iodides which is in agreement with the previously reported results for a CH_3I treated catalyst.[5]

The use of bromomethane for longer gas phase treatments has been reported previously and showed no significant difference compared with iodomethane in the ability to disperse the gold particles.[4] Fig. 2 reports the results for gas phase treatments using *n*-bromobutane, *n*-bromohexane and *n*-bromooctane. Whilst the XRD pattern for the catalyst treated with *n*-bromobutane did not show a significant change in the gold features, treatment with both *n*-bromohexane and *n*-bromooctane showed almost complete disappearance of the gold peaks.

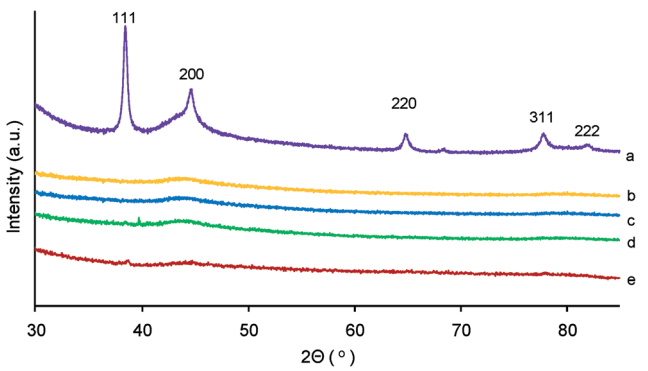

Fig. 1 XRD of Au/C catalysts (a) as received and after treatment with gas phase (b) iodomethane, (c) *n*-iodobutane, (d) *n*-iodohexane and (e) *n*-iodooctane at 240 °C for 1 h.

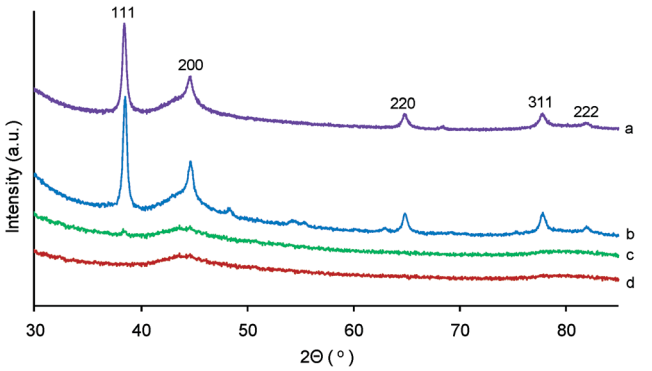

Fig. 2 XRD of Au/C catalysts (a) as received and after treatment with gas phase (b) *n*-bromobutane, (c) *n*-bromohexane, (d) *n*-bromooctane at 240 °C for 1 h.

The treatment with gaseous halo compounds has the potential to leach gold from the support into the vapour phase in the form of volatile gold complexes. To check for loss of gold, ICP-OES analysis was undertaken before and after treatment. Table 3 summarises the amount of gold in the as received and treated samples. From these results it is clear for all the gas phase treated samples that the gold is still present. In the case of the iodoalkanes, a decrease of up to 20% of the gold was observed which may be associated with volatilisation of the gold. In the case of the bromoalkanes, there was a greater reduction in the gold content which may be due to the likely higher volatility of the bromine based complexes than the analogous iodine based ones due to their lower molecular weight. However, given that there is still a significant presence of gold after the treatments, the disappearance of the gold features in the X-ray diffractograms for the treated samples is consistent with re-dispersion of gold into smaller sized particles rather than removal of gold, predominantly.

Pure liquid phase halohydrocarbon treatments

The X-ray diffractograms of the catalyst samples treated with pure liquid phase iodohydrocarbons are reported in Fig. 3.

As found for the gas phase treatment, the liquid phase treatment led to complete removal of the gold features in the case of *n*-iodobutane, *n*-iodohexane and *n*-iodooctane with some features remaining, albeit much smaller, in the

Table 3 ICP-OES analysis of Au/C catalysts after treatment with gas phase iodoalkanes

Treatment	Au (wt.%)
As received	1.02
Iodomethane (g)	1.01
n-Iodobutane (g)	0.93
n-Iodohexane (g)	0.82
n-Iodooctane (g)	0.81
n-Bromobutane (g)	0.56
n-Bromohexane (g)	0.57
n-Bromooctane (g)	0.54

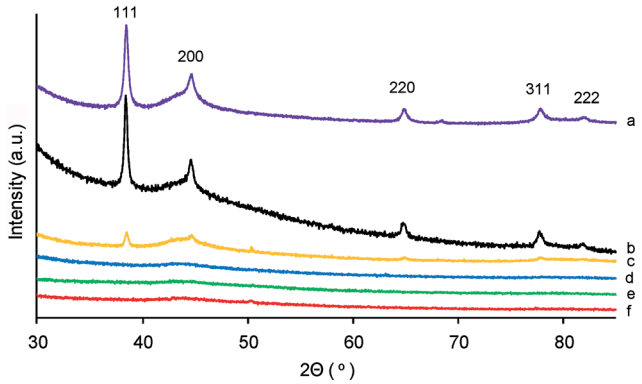

Fig. 3 XRD of Au/C catalyst (a) as received and after treatment in the liquid phase using pure (b) *p*-iodotoluene, (c) iodomethane, (d) *n*-iodobutane, (e) *n*-iodohexane and (f) *n*-iodooctane at 40 °C for 1 h.

case of iodomethane. Interestingly, for the iodomethane, little change in the particle size is found for the gold which can be observed using XRD with the full width half maximum (FWHM) of the Au(111) feature being 0.36° compared with 0.41° for the as received catalyst. This is consistent with the mechanism of the gold dispersion proposed previously whereby the gold particles are etched rather than broken into smaller and smaller fragments.[1,5] In the case of the treatment with *p*-iodotoluene no significant change was observed in the XRD pattern.

In the case of the liquid phase treatment using the equivalent bromohydrocarbons (Fig. 4), no gold diffraction features were observed using *n*-bromohexane and *n*-bromooctane. For *n*-bromobutane, some decrease in the intensities of the Au diffraction features was observed. Again, as found with iodomethane, the full width half maximum was similar to the as received catalyst samples at 0.32° (Au(111)) for the sample treated with *n*-bromobutane. In agreement with the treatment with *p*-iodotoluene, the use of *p*-bromotoluene did not lead to any changes in the X-ray diffractogram.

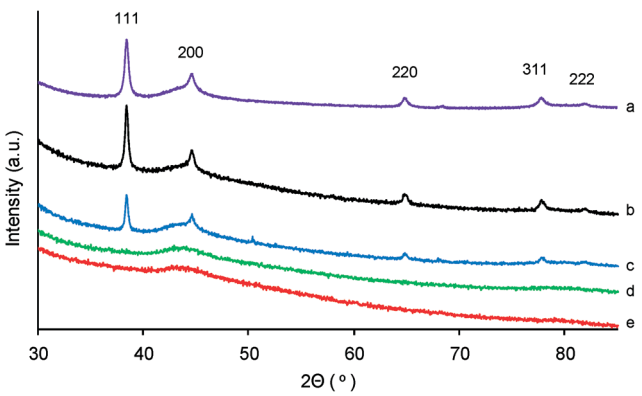

Fig. 4 XRD of Au/C catalyst (a) as received and after treatment in the liquid phase using pure (b) *p*-bromotoluene, (c) *n*-bromobutane, (d) *n*-bromohexane and (e) *n*-bromooctane at 40 °C for 1 h.

Table 4 ICP-OES Analysis of Au/C catalysts after treatment with liquid phase halohydrocarbons in the pure and diluted forms. The gold content of the as received catalyst was 1.02 wt.% (Table 3)

	Au (wt.%)	
Treatment	Pure	Dilute
Iodomethane	0.75	0.60
n-Iodobutane	0.85	0.80
n-Iodohexane	0.67	0.71
n-Iodooctane	0.79	0.78
p-Iodotoluene	0.41	0.42
n-Bromobutane	0.79	0.79
n-Bromohexane	0.68	0.71
n-Bromooctane	0.77	0.70
p-Bromotoluene	0.50	0.50

Table 4 summarises the gold content determined by ICP-OES following the treatment with the pure liquid halohydrocarbons. In the case of the halotoluene compounds, there is a reduction in Au wt.% of at least 50%. Given that the XRD of the samples treated with the halotoluenes remain relatively unchanged from the fresh sample this may be associated with removal of weakly bound particles from catalyst support without reacting with the more strongly bound gold nanoparticles. In all other cases, some removal of weakly bound gold is also found, as observed by the decrease in gold content of between 15 and 33%; however, in these cases, the remaining gold reacts and forms highly dispersed nanoparticles, as confirmed in the HAADF-STEM studies. An additional benefit which the use of the liquid systems has over the original gas phase treatment is that, in the event of the reduction of gold content on the catalyst, recovery of any gold leached from the catalyst would be much more readily achieved. Furthermore, it is apparent that there is much smaller reduction in gold content in the case of the liquid phase bromoalkane treatments when compared with the analogous gas phase treatments.

Fig. 5 reports the HAADF-STEM image and the particle size distribution of 400 particles observed in the as received Au/C catalyst. Large gold nanoparticles are found with an average particle size around 27 nm and a dispersion of 3.3%. HAADF-STEM studies of the pure *n*-iodomethane, *n*-iodobutane and *n*-iodohexane treated samples showed

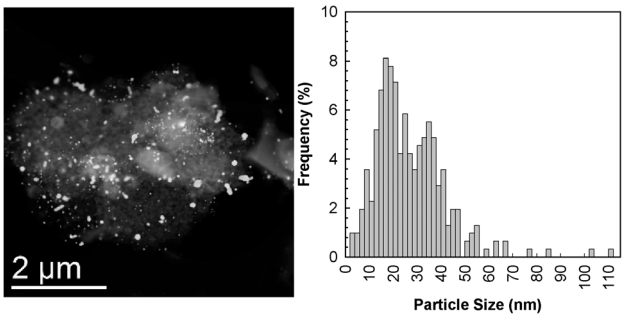

Fig. 5 HAADF image (left) and particle size distribution (right) of the as received Au/C catalyst.

that following the treatment the gold nanoparticles are re-dispersed (see Fig. 6).

In the case of the *n*-iodomethane some large particles (up to 50 nm) were still observed. However, 95% of the counted particles were smaller than 2 nm. In the case of the *n*-iodobutane and *n*-iodohexane treated samples, no particles larger than 1.25 nm were observed. In fact, the particle size was so close to the resolution limit of the equipment (0.5 nm) showing that the presence of even smaller gold clusters cannot be excluded. It should be pointed out that particles which are smaller than 0.75 nm consist of less than 10 gold atoms, showing the high efficiency of the method described, herein.

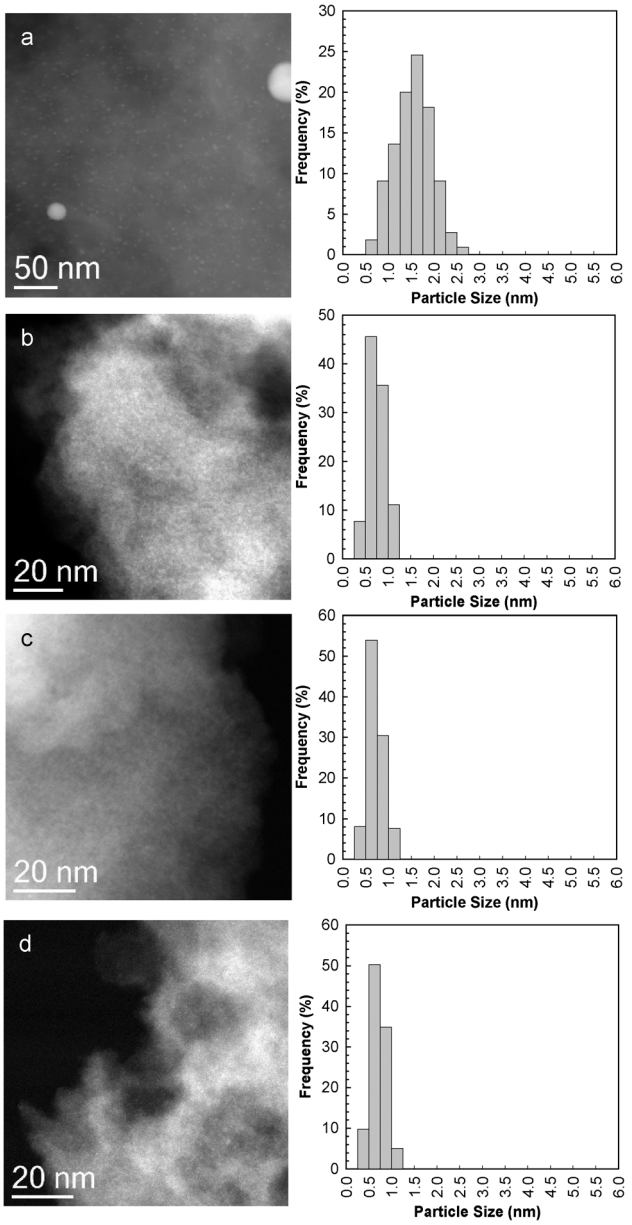

Fig. 6 Typical HAADF image (left) and particle size distribution (right) of Au/C catalysts after the liquid phase treatment with pure *n*-iodomethane (a), *n*-iodobutane (b), *n*-iodohexane (c) and *n*-iodooctane (d).

Table 5 Content of Au/C catalysts obtained by EDX after the respective re-dispersion treatments

	Au : X molar ratio	
Treatment	Pure	Dilute
Iodomethane	0.2	—
n-Iodobutane	0.1	0.1
n-Iodohexane	0.1	0.2
n-Iodooctane	0.1	0.1
n-Bromobutane	0.3	—
n-Bromohexane	0.3	—
n-Bromooctane	0.2	—

Table 5 includes the molar ratio of gold to halogen the samples after the treatments (as determined by EDX). A high concentration of iodine was observed on the sample after treatment with pure liquid iodoalkanes, and as such a low Au : I molar ratio was observed. Mole ratios of between 0.1 and 0.2 Au : I were observed for the treated samples. This is in agreement with the mechanism of the gold dispersion whereby the halogen stabilises the gold clusters forming $(Au_yI_z)^{a+}$.

Fig. 7 shows the results of the HAADF-STEM for the pure *n*-bromobutane, *n*-bromohexane and *n*-bromooctane treated samples. In the cases of the pure *n*-bromobutane and *n*-bromohexane treated samples, although some large gold particles still remained, the majority of the gold had been re-dispersed to give much smaller gold nanoparticles. With the *n*-bromobutane treated sample the majority of the gold particles were smaller than 3 nm, with an average size of 1.5 nm and a dispersion of 55%. In the case of the *n*-bromohexane treated sample, the majority of the particles were smaller than 2.5 nm, with an average particle size of 1.2 nm and 59% dispersion. In the case of the pure *n*-bromooctane treated samples, no large particles were observed. After counting 125 particles, the largest particle that was observed was 1.5 nm, and the average size was 1.0 nm. Bromine was also found on the samples. In general, the molar ratio of Au : Br is larger than that observed in the case of the Au : I molar ratio of the pure iodohydrocarbon treated samples (see Table 5).

Ideally, for the catalytic application of gold, it is important to reduce the amount of halide in the samples post-treatment. A hydrothermal treatment has previously been reported as successful for the removal of iodine.[5] These experiments consisted of flowing 10% H_2/Argon (20 cm^3 min^{-1}) through a H_2O saturator and then through the sample held in a quartz tube which was heated by a furnace at 190 °C for at least 15 min. These conditions have been applied, in this study, for 30 min to the catalysts treated with the pure bromohydrocarbons in the liquid phase. A comparison of the ICP-OES results (see Table 6) of the halohydrocarbon treated materials and those post hydrothermal treatment showed the complete removal of bromine (to less than the detection level of the instrument) while the Au wt.% has remained relatively unchanged. Furthermore, XRD analysis after these treatments has shown that there is no change in the diffractogram of the respective samples when comparing pre and post hydrothermal treatment. Hence it is

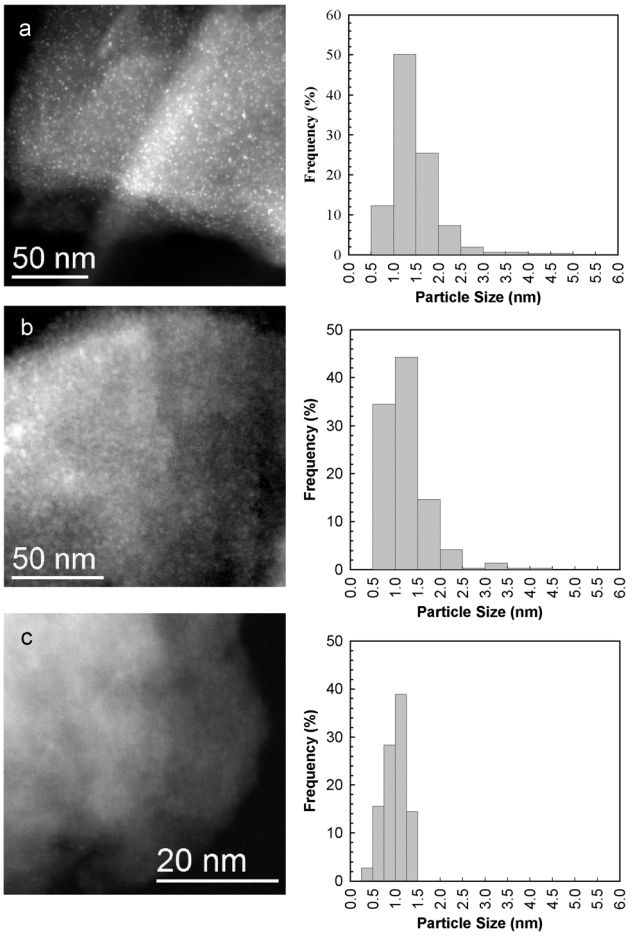

Fig. 7 Typical HAADF-STEM image (left) and particle size distribution (right) of Au/C catalysts after treatment with pure *n*-bromobutane (a), *n*-bromohexane (b) and *n*-bromooctane (c).

Table 6 ICP-OES analysis of pure bromoalkane treated Au/C catalysts, before and after hydrothermal treatment

	Before	After
Sample	Br (wt.%)	Br (wt.%)
n-Bromobutane	1.0	<0.05
n-Bromohexane	4.2	<0.05
n-Bromooctane	3.9	<0.05

believed that the gold particle size remains relatively unchanged after such hydrothermal treatments.

Table 7 compares the average particle size for the bromoalkane treated samples with those treated with iodoalkanes. In general, comparing the butyl, hexyl and octyl species, the iodoalkane treated samples have smaller particles (0.6 to 0.7 nm) than the bromoalkane samples (1.0 to 1.5 nm).

Whilst there is a drop in the gold content of the catalyst following the halohydrocarbon treatment this is more than offset by the increase in the available surface area. Assuming a cuboctahedron particle shape for the gold nanoparticles, the relative surface areas of the gold for 27 nm and 1.5 nm particles for the same total gold loading is 18 times higher

Table 7 Average particle size after the respective pure haloalkane re-dispersion treatments; volume and surface area for particles of these average sizes and comparison of total gold surface area

Treatment	Average particle size (nm)
As received	27.0
Iodomethane	1.4
n-Iodobutane	0.6
n-Iodohexane	0.7
n-Iodooctane	0.6
n-Bromobutane	1.5
n-Bromohexane	1.2
n-Bromooctane	1.0

for the smaller particles. Therefore, even with the 46% reduction in gold content, this re-dispersion would still result in an increase in the surface area of almost 10 times. Given that 1.5 nm was the largest average particle size observed after the treatments with the halo hydrocarbons, it is apparent that for the smaller average particle sizes the increase in total surface area of the gold particles will be even larger and is up to 45 times for the particles of 0.6 nm in size. A comparison of surface areas and volumes for all the observed average particle sizes can be found in the ESI.†

Dilute liquid phase halohydrocarbon treatments

Fig. 8 shows the changes in the X-ray diffractograms as a function of the treatment with diluted iodohydrocarbons in the liquid phase. No significant changes in the diffractograms for diluted iodomethane, *n*-iodobutane or *p*-iodotoluene were observed when compared with the as received catalyst. However, following treatment in *n*-iodooctane, no gold features were observed. In addition, there was a decrease in intensity of gold features observed for the *n*-iodohexane treatment. In all cases, there was little variation in the full width at half maximum. Table 3 also shows the concentration of gold remaining following the treatments. With the exception of the iodomethane treated material, all samples showed similar levels of leaching compared with the pure treated samples.

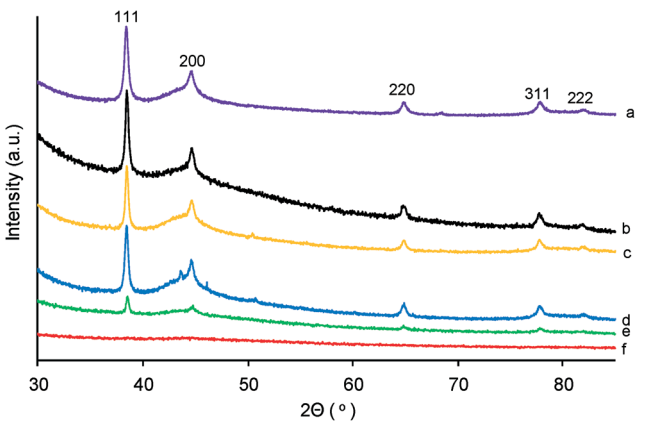

Fig. 8 XRD of Au/C of the (a) as received catalyst and following treatment with dilute iodohydrocarbon (b) *p*-iodotoluene, (c) iodomethane, (d) *n*-iodobutane, (e) *n*-iodohexane and (f) *n*-iodooctane.

In the case of dilute bromo hydrocarbon treatments no discernible changes in XRD pattern were observed when compared with the as received catalyst.

HAADF-STEM was also conducted for these dilute RI treated samples. As expected from the XRD patterns the extent of re-dispersion over these samples was limited compared with the corresponding pure liquid RI treatments. For this reason, there is heterogeneity in terms of shape and size of the gold particles of the dilute RI treated samples making it difficult to obtain an accurate particle size distribution.

A typical HAADF-STEM image for the dilute *n*-iodooctane sample is reported in Fig. 9, from which it is apparent that a significant amount of dispersion has occurred, albeit to a lesser extent than that observed for the corresponding pure iodoalkane treatments. In addition, the amount of iodine observed in the samples by EDX after the treatments is smaller than that observed in the case of the pure halohydrocarbon compounds (see Table 5).

Following treatment with the dilute *n*-iodooctane and *n*-bromooctane, the liquid phase was analyzed by GCMS to identify any molecules formed as a result of the reaction with the gold. The analysis did show the presence of small quantities of the C_8H_{17} coupling, *i.e.* $C_{16}H_{34}$ in the case of *n*-iodooctane; however, this was in such small concentration that accurate quantification was not possible. Although further investigation is still required in terms of the mechanism, these GCMS results would support, in the case of *n*-iodooctane treatment, the previously proposed mechanistic route where the haloalkanes dissociatively react with the gold forming a higher molecular weight alkane, see eqn (1) for the treatment with *n*-iodooctane.[1,5]

$$2C_8H_{17}I + Au_X = (Au_yI_z)^{a+} + C_{16}H_{34} \quad (1)$$

A time course study of the diluted *n*-iodooctane treatments was conducted with a view to examine the change in full width half maximum with time and an optimisation of the method to enable control of the particle size using time/concentration of the dispersant as the variables.

Fig. 10 shows the variation in the XRD patterns of the Au/C as a function of the treatment time and Fig. 11 shows how the normalised intensities of the Au(111) peak changes

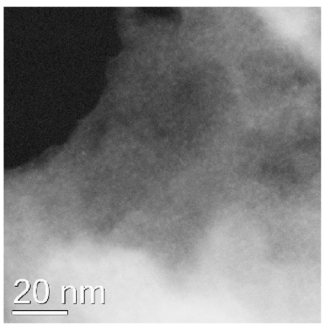

Fig. 9 HAADF-STEM image of Au/C after treatment with dilute *n*-iodooctane.

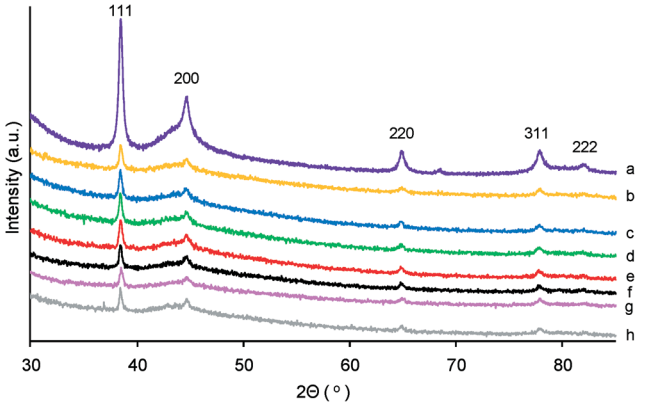

Fig. 10 XRD of the Au/C catalyst as a function of time of treatment with dilute liquid phase *n*-iodooctane after (a) 0 h, (b) 2 h, (c) 4 h, (d) 8 h, (e) 12 h, (f) 16 h, (g) 20 h and (h) 24 h.

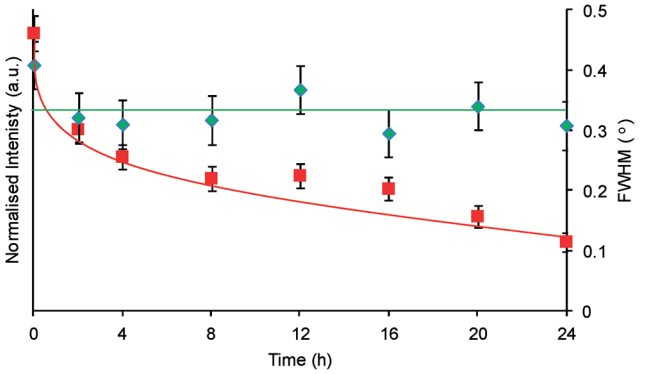

Fig. 11 Variation in the peak height normalised to background/support intensity (■) and FWHM (♦) of the Au(111) peak at ~38.4°, as a function of time during the liquid phase treatment of Au/C using diluted *n*-iodooctane.

(the error in the signal is equivalent to 3.85%). A gradual decrease in the intensity of the gold features is observed. However, as found with other treatments which showed gold peaks following the treatment (Fig. 2, 3, 4 and 8), little change in the particle size is found for the gold which can be observed using XRD, with the full width half maximum of the Au(111) remaining relatively unchanged, as reported in Fig. 11.

Again, this is consistent with the mechanism of the gold dispersion proposed previously whereby the gold particles are etched rather than fragmented.[1,5] ICP-OES analysis was utilised to confirm that there was still a significant amount of Au present (see Table 8). Although there is a loss of gold in all of the samples, there is still a significant amount present (~0.7% compared with 1.02% in the case of the as received sample). Interestingly, the gold leaching after 2 h treatment is similar to that found after 24 h. This may indicate that the initial contact with the liquid phase hydrocarbon removes weakly bound gold and, thereafter, reacts with the more strongly bound gold leading to re-dispersion. This is consistent with the proposed reason for the leaching associated with the

Table 8 ICP-OES analysis of Au/C catalyst as a function of time of liquid phase treatment using dilute *n*-iodooctane

Time (h)	Au wt.%
0	1.02
2	0.70
4	0.75
6	0.74
8	0.71
12	0.72
16	0.71
20	0.74
24	0.70

Table 9 ICP-OES analysis of Au/C catalysts treated with solvent

Solvent	Au wt.%
Water	0.71
Acetonitrile	0.64
Hexane	0.69
Toluene	0.60

haloaromatics where reaction/dispersion did not occur but a drop in the gold content was observed (Table 3).

The existence of weakly bound gold is supported by the variation in the gold content following washing the catalyst with water, acetonitrile, hexane and toluene in the absence of any halohydrocarbons. Table 9 compares the gold contents as obtained from ICP-OES following the treatments. Significant reductions in gold content were observed of up to 40%. Following these treatments no change in the XRD patterns were observed indicating no significant reduction in the gold particle size. The decreases in gold content observed are similar to those found when initially treated with the halohydrocarbon and are, therefore, not thought to be associated with any reaction with the gold.

The variation between the ability of the aromatic and aliphatic halohydrocarbons may be attributed to the significantly higher R–X bond strengths for *p*-iodotoluene and *p*-bromotoluene compared with the equivalent aliphatic compounds.[15] This explanation may also provide an explanation for the ability of iodo compounds to disperse the gold more easily than the analogous bromo compounds. For example, in the case of *n*-iodobutane, the R–I bond dissociation energy is 226.4 kJ mol^{-1}, compared with 296.6 mol^{-1} for the R–Br bond of *n*-bromobutane.[15] Although the variation of the bond strengths within the family of iodoalkanes or bromoalkanes is much smaller[15–17] it has been reported that R–X bond fission reduction potentials of straight chained organo halide compounds decreased as the carbon chain length increased[18,19] which may also explain the ability to control the dispersion.

For the variation in the bromo and iodo compounds it may also be the case that the stability of the gold final state controls some of the particle size variation. The bond strength of Au–I is much higher than for Au–Br (276 kJ mol^{-1} *vs.* 213 kJ mol^{-1})[20] which may lead to smaller particles overall for the former treatment, as observed from the electron microscopy. Interestingly, this change in the gold-halogen bond strength may be of additional benefit since the bromine is likely to be easier to be removed and so the use of the bromoalkanes could enable the catalyst to be cleaned more easily after treatment.

Conclusions

This work demonstrates the possibility of using different haloalkanes to replace iodomethane for the re-dispersion of gold nanoparticles in supported gold catalysts. From these experiments, an alternative method of treatment has been established through the use of liquid systems. An additional benefit of the use of the liquid systems is that in the event of loss of gold from the catalyst, it should be much easier to recover from the solution used for the re-dispersion treatment. Furthermore, by using the dilute system it may be possible to obtain greater control over the gold particle re-dispersion and hence tune the process to yield the most desirable gold particle size.

Acknowledgements

We gratefully acknowledge funding for this work from King Abdulaziz University (grant no. D-005/431), and the CASTech grant (EP/G012156/1) from the EPSRC.

Notes and references

1 J. Sá, R. Taylor, H. Daly, A. Goguet, R. Tiruvalam, Q. He, C. J. Kiely, G. J. Hutchings and C. Hardacre, *ACS Catal.*, 2012, **2**, 552.
2 M. Haruta, T. Kobayachi, H. Sano and N. Yamada, *Chem. Lett.*, 1987, **2**, 405.
3 G. J. Hutchings, *J. Catal.*, 1985, **96**, 292.
4 A. Goguet, C. Hardacre, I. Harvey, K. Narasimharao, Y. Saih and J. Sá, *J. Am. Chem. Soc.*, 2009, **131**, 6973.
5 J. Sá, S. F. R. Taylor, C. Paun, A. Goguet, R. Tiruvalam, C. J. Kiely, M. Nachtegaal, G. J. Hutchings and C. Hardacre, *Angew. Chem., Int. Ed.*, 2011, **50**, 8912.
6 A. Abad, P. Concepcion, A. Corma and H. Garcia, *Angew. Chem., Int. Ed.*, 2005, **44**, 4066.
7 S. Biella and M. Rossi, *Chem. Commun.*, 2003, 378.
8 J. Guzman and B. C. Gates, *J. Am. Chem. Soc.*, 2004, **126**, 2672.
9 J. R. Zoeller, A. H. Singleton, G. C. Tustin and D. L. Carver, U.S. Patents Nos. 6,506,933 and 6,509,293, 2003.
10 Recommendation from the Scientific Committee on Occupational Exposure Limits for methyl iodide, European Commission, 1999.
11 L. A. Poirier, G. D. Stoner and M. O. Shimkin, *Cancer Res.*, 1975, **35**, 1411.
12 N. I. Sax and R. J. Lewis, *Dangerous Properties of Industrial Materials*, 1989, Van Nostrand Reinhold, New York, USA.

13 Sigma Aldrich Material Safety Data Sheets for RX compounds, 2011 to 2012.
14 Derived from Sigma Aldrich online catalogue, accessed November 2013.
15 Y. R. Luo, *Bond Dissociation Energies in Organic Compounds*, CRC Press, Boca Raton, Florida, USA, 2003.
16 R. T. Sanderson, *Chemical Bonds and Bond Energy*, Academic Press, New York, USA, 1974.
17 T. L. Cottrell, *The Strengths of Chemical Bonds*, Butterworths, London, UK, 1958.
18 I. Rosenthal, C. H. Albright and P. J. Elving, *J. Electrochem. Soc.*, 1952, **99**, 227.
19 P. J. Elving, J. M. Markowitz and I. Rosenthal, *J. Electrochem. Soc.*, 1954, **101**, 195.
20 Y. R. Luo, *Comprehensive Handbook of Chemical Bond Energies*, CRC Press, Boca Raton, Florida, USA, 2007.